EPJ AP

Applied Physics

EPJ.org your physics journal

Eur. Phys. J. Appl. Phys. (2014) 67: 21301 DOI: 10.1051/epjap/2014140191

# Depth profiling and morphological characterization of AlN thin films deposited on Si substrates using a reactive sputter magnetron

Carlos Macchi, Juan Bürgi, Javier García Molleja, Sebastiano Mariazzi, Mattia Piccoli, Edoardo Bemporad, Jorge Feugeas, Roberto Sennen Brusa, and Alberto Somoza

The title "The European Physical Journal" is a joint property of EDP Sciences, Società Italiana di Fisica (SIF) and Springer

Eur. Phys. J. Appl. Phys. (2014) 67: 21301
DOI: 10.1051/epjap/2014140191

THE EUROPEAN PHYSICAL JOURNAL
APPLIED PHYSICS

Regular Article

# Depth profiling and morphological characterization of AlN thin films deposited on Si substrates using a reactive sputter magnetron

Carlos Macchi[1], Juan Bürgi[2], Javier García Molleja[2,a], Sebastiano Mariazzi[3], Mattia Piccoli[4], Edoardo Bemporad[4], Jorge Feugeas[2], Roberto Sennen Brusa[5], and Alberto Somoza[6]

[1] IFIMAT, UNCentro and CONICET, Pinto 399, B7000GHG Tandil, Argentina
[2] Instituto de Física Rosario, CONICET-UNR, Bvrd. 27 de Febrero 210 Bis, S2000EZP Rosario, Argentina
[3] Dipartimento di Fisica, Università di Trento and INFN, Gruppo collegato di Trento, Via Sommarive 14, 38123 Povo, Trento, Italy
[4] Dipartimento di Ingegneria Meccanica ed Industriale (DIMI), Università di Roma Tre, Via della Vasca Navale 79, 00146 Rome, Italy
[5] Dipartimento di Fisica and CNISM, Università di Trento, Via Sommarive 14, 38123 Povo, Trento, Italy
[6] IFIMAT, UNCentro and CICPBA, Pinto 399, B7000GHG Tandil, Argentina

Received: 7 May 2014 / Received in final form: 12 June 2014 / Accepted: 13 June 2014
Published online: 1 August 2014 – © EDP Sciences 2014

**Abstract.** It is well-known that the characteristics of aluminum nitride thin films mainly depend on their morphologies, the quality of the film-substrate interfaces and the open volume defects. A study of the depth profiling and morphological characterization of AlN thin films deposited on two types of Si substrates is presented. Thin films of thicknesses between 200 and 400 nm were deposited during two deposition times using a reactive sputter magnetron. These films were characterized by means of X-ray diffraction and imaging techniques (SEM and TEM). To analyze the composition of the films, energy dispersive X-ray spectroscopy was applied. Positron annihilation spectroscopy, specifically Doppler broadening spectroscopy, was used to gather information on the depth profiling of open volume defects inside the films and the AlN films-Si substrate interfaces. The results are interpreted in terms of the structural changes induced in the films as a consequence of changes in the deposition time (i.e., thicknesses) and of the orientation of the substrates.

## 1 Introduction

Aluminum nitride (AlN), which belongs to type III-V family of semiconductor compounds, can give zinc-blend (fcc) or wurtzite (hcp) crystalline structures, being wurtzite the only thermodynamically stable structure. Wurtzitic AlN (theoretical density equal to 3.26 g/cm$^3$) has a wide electronic band-gap, possesses good piezoelectric response, high electrical resistivity, high breakdown voltage, high acoustic propagation rate with low transmission losses, high thermal conductivity, high chemical stability, high resistance to corrosion and high hardness [1].

As a thin film, AlN is an excellent piezoelectric material [2] for surface acoustic wave (SAW) devices [3,4], and can be used as bulk acoustic wave (BAW) filter [5]. Besides, these films can be used in microelectromechanics systems (MEMS) applications like micromotors, micropumps or accelerometers [6,7], and as chemical and biological sensors [8,9]. But as micrometric films, AlN is also used as hard coating in tribological applications [10].

Nevertheless, the characteristics of AlN films strongly depend on their morphologies. They can be developed as nanometric monocrystalline films by epitaxial growing or nano- or micrometric polycrystalline films with different grain sizes using plasma enhanced chemical vapor deposition (PECVD) or plasma enhanced physical vapor deposition (PEPVD) techniques. Among PEPVD techniques, reactive sputter magnetron (RSM) is the most extensively used and precisely it was used in the present work. The films prepared by RSM may have different textures inducing different piezoelectric polarities [5].

RSM deposition has several important advantages in producing thin films [11]. It is capable of producing films of compounds with controllable stoichiometry and at high deposition rates, even at industrial scale. By means of RSM it is possible to obtain high purity films at deposition temperatures below 300 °C [12]. Composition, structure and quality of the films depend on an important number of

[a] e-mail: garciamolleja@ifir-conicet.gov.ar

physical and geometrical parameters associated with the process. Recently, Kale et al. [13] used an AlN target to deposit AlN films on copper, quartz and silicon substrates by means of RF magnetron sputtering technique. These authors studied the effect of deposition conditions on the structural and electrical properties of the films.

In literature, an important number of authors have reported results of different morphological studies on wurtzitic AlN polycrystalline thin films grown with or without well-defined preferential crystalline planes of orientation. These observations were principally obtained using X-ray diffraction (XRD); in the resulting diffractograms, peaks with higher intensities according to certain specific crystalline planes were observed. These preferential orientations can give non-polar as $(1\,0\,\bar{1}\,0)$ and $(1\,1\,\bar{2}\,0)$, semi-polar as $(1\,0\,\bar{1}\,1)$ or polar $(0\,0\,0\,2)$ textures which are more linked to the deposition mechanism than to the influence of the crystal structure of the substrate [14]. For example, some authors have found that by changing the magnetron target-substrate distance, it is possible to obtain AlN thin films with different preferential orientations, like $(0\,0\,0\,2)$ or $(1\,0\,\bar{1}\,0)$ [10]. On the other hand, other authors found similar results but through the modification of the working pressure of the reactive gas mixtures used in the deposition process [12].

Independently of the deposition process, the nature and quality of the films depend on: the size of the single crystals; the columnar structure; the density; and the quality of the substrate-film interface [15].

In the present work, we have studied morphological characteristics of AlN thin films deposited by RSM on Si substrates with different orientations. The analysis of the films was carried out using X-ray diffraction, scanning electron microscopy and Doppler broadening spectroscopy (DBS). The obtained results are of utmost importance when AlN films are intended to be used to fabricate coatings for tribological applications [10].

## 2 Experimental

The deposition of AlN on Si was carried out using a reactive sputter magnetron with an 8 $cm^2$ high purity aluminum target and the silicon substrates were placed at 50 mm from the target. Prior the film deposition, and to take away the superficial alumina, the Al target was cleaned by sputtering with Ar for 10 min. The deposition working conditions consisted of a DC voltage of 260 V applied to the magnetron in order to induce a current of 208 mA; thus, the resulting density of power on the magnetron was of 6.76 $W/cm^2$. This process was sustained in a reactive gas atmosphere at a total pressure of 4 mbar consisting of a mixture of Ar (67%) and $N_2$ (33%) with controlled fluxes of 16 and 8 sccm, respectively. These operating conditions were established during 15 min with the surface of the substrate covered with a shutter; in this time the stable conditions of the discharge were reached. Then, the shutter was removed and the substrate surface was exposed to the AlN deposition during selected times; in our case, 20 and 30 min, respectively.

Samples with AlN films depositions were studied using XRD in a $\theta/2\theta$ configuration which makes it possible to determine the crystalline structure. To this aim, a diffractometer with a Cu K$\alpha_1$ source (at 40 kV and 30 mA) with a resulting X-ray wavelength of 1.54 Å was used. The X-ray beam was collimated by a couple of Soller slits obtaining an X-ray beam cross section of $4 \times 4$ $mm^2$. $2\theta$ reflected angles were monitored between 30° and 60° with steps of 0.03° every 1 s.

Film cross sections were also examined by scanning electron microscopy (SEM) and transmission electron microscopy (TEM), using foil cut with the focused ion beam (FIB) lamellae method. Energy-dispersive X-ray spectroscopy (EDS) analysis was used to monitor the composition of the films.

DBS measurements were performed with an electrostatic slow positron ($e^+$) beam at the Trento University [16,17]. The beam was tunable in the 0.05–25 keV energy ($E$) range. These positron implantation energies correspond to a probed film thickness ranging from ≈0.3 nm to about 2 $\mu$m in AlN samples. The positron beam was coupled to two high purity germanium detectors (HPGe), 45% efficiency, 1.4 keV resolution at 511 keV, in a 180° configuration. At each positron implantation energy, the 511 keV gamma line was acquired with a microspectrum method and stabilized by a software procedure [18].

Positrons injected in a solid with energy ranging from a few eV to some keV slow down in few picoseconds (1–3 ps at 300 K) reaching thermal energies inside material. For monoenergetic positrons, the stopping profile can be well-described by a derivative of a Gaussian function [19,20]. The mean stopping depth $\langle z \rangle$ is related to the positron implantation energy $E$ by the equation:

$$\langle z \rangle = \frac{40}{\rho} E^{1.6} \text{ nm}, \quad (1)$$

where $E$ is expressed in keV and the material density $\rho$ in g $cm^{-3}$ [20,21]. Then, after diffusion path positron annihilates into two 511 keV $\gamma$-rays with an electron of the medium.

When using DBS the 511 keV annihilation peak is usually characterized by two line shape parameters $S$ and $W$. The shape parameter $S$ represents the fraction of positrons annihilating with low-momentum electrons and it is defined as the ratio between the counts in a central area of the annihilation peak, $|511 - E_\gamma| \leq 0.85$ keV, and the counts in the total area of the peak, $|511 - E_\gamma| \leq 4.25$ keV. The wing parameter $W$ represents the fraction of positrons annihilating with high-momentum electrons, it is defined as the ratio between the counts in the wing regions of the annihilation peak, 1.6 keV $\leq |511 - E_\gamma| \leq$ 4 keV, and the counts in the total area of the peak. The narrowing of the 511 keV annihilation line indicates that more positrons are annihilating with electrons of low momentum; this behavior is reflected in an increase of the $S$ values and a decrease of the $W$ ones, respectively.

From the DBS spectra, the $S$ and $W$ parameters were estimated with a statistical error about 0.1% (more than $2.5 \times 10^5$ counts under each annihilation spectrum).

**Table 1.** Experimental details of the different samples studied. The thicknesses values reported were measured by SEM.

| Sample | M1-20 | M0-20 | M1-30 | M0-30 |
|---|---|---|---|---|
| Substrate monocrystal | Si (1 1 1) | Si (1 0 0) | Si (1 1 1) | Si (1 0 0) |
| Deposition time (min) | 20 | 20 | 30 | 30 |
| AlN film thickness (nm) | 230 | 200 | 390 | 260 |
| AlN-Si interface thickness (nm) | 35 | 28 | 30 | 36 |

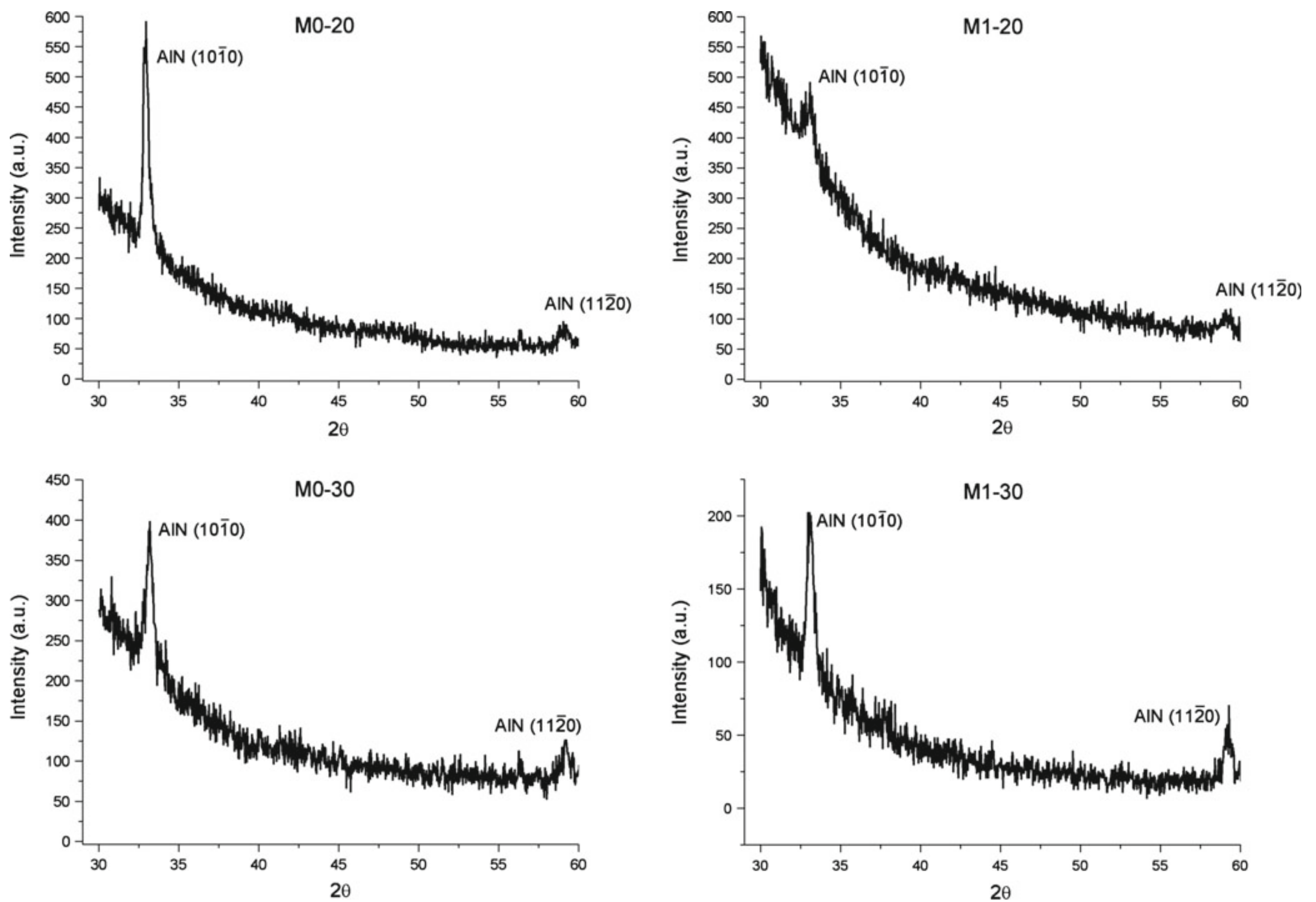


**Fig. 1.** X-ray diffractograms for the four AlN thin films analyzed.

Usually, to analyze DBS data shape line parameters are normalized to that of bulk Si ($S_b$ and $W_b$, respectively); that is $S_n = S/S_b$ and $W_n = W/W_b$. In this work, pure Si was used as substrate material (i.e., substrate bulk $\equiv$ Si bulk).

## 3 Results and discussion

In the present work, 0.6 mm thickness of (1 1 1) and (1 0 0) monocrystalline Si samples were used as substrates, respectively. The AlN deposition was carried out to produce films with thicknesses that also make it possible to explore the film-substrate interfaces. In fact, taking into account the typical mean depth penetration of positrons in solids, all films were fabricated with a thickness approximately 300 nm. This thickness was enough to ensure a well developed AlN crystalline structure. The films were deposited during 20 and 30 min on each type of Si substrate using the physical and geometrical conditions described in Section 2. For clarity purposes, the different samples were labeled as reported in Table 1.

Figure 1 shows XRD results corresponding to the four samples indicated in Table 1. Such diffractograms show the existence of a polycrystalline structure with two peaks corresponding to the hcp non-polar crystalline planes $(1\,0\,\bar{1}\,0)$ and $(1\,1\,\bar{2}\,0)$ of wurtzitic AlN [12]. As can be seen, the intensities of the peaks are weak and they are also accompanied by an appreciable background which can be attributed to the low thickness of the films.

In Figure 2, a cross section TEM micrograph of the sample M1-30 is shown. In the image, the following was observed: the film is constituted by an AlN polycrystalline layer [22] with a columnar structure (named layer I) with

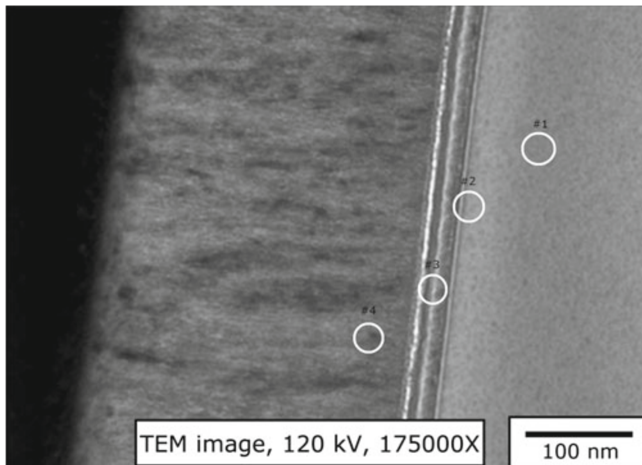


**Fig. 2.** Cross section TEM micrograph of the sample M1-30. In this image, it can be seen: the columnar structure of AlN on the left part of the image (layer I), the interface in the center (layer II) and the Si (1 1 1) substrate on the right. Lines with different degrees of brightness at the interface correspond to an effect of the cutting process during the preparation of the sample. Numbered circles indicate the regions in which EDS measurements were carried out.

a thickness around 350 nm, and a thinner amorphous interface (named layer II) with a thickness about 35 nm. The lines with different degrees of brightness parallel to the surface of the interface can be attributed to the transversal cutting process during the preparation of the sample.

As an example of the AlN films prepared, in Figure 3 two cross section SEM micrographs of the samples are shown. One corresponds to 20 min of deposition time (sample M0-20) and the other to 30 min (sample M0-30). The columnar structure of the AlN films is evident in the TEM and SEM images. This structure does not change with the deposition time or the orientation of the substrate [23]. The columns have typical sizes between 15 and 20 nm. For all the measured samples, the thicknesses of the films have been measured from the SEM images; the obtained values are reported in Table 1.

To go further into the analysis of the composition of the film and substrate-film interfaces, EDS spectra were recorded in different regions of the samples. In Figure 2, these regions are stressed with circles that indicate the substrate (label # 1), the interface near substrate (label # 2), the interface (label # 3) and the first atomic layers of the deposited AlN film (label # 4), respectively. In Table 2, the element concentrations in the regions selected in Figure 2 are reported.

Specifically, EDS measurements were performed with an angle of incidence of the electron probe perpendicular to the film cross section. The element concentration corresponding to the deposited AlN bulk was determined from several EDS area analysis. In order to obtain information on an enlarged volume of the bulk, EDS measurements were made using a low electron energy in the beam (with a voltage of 7 kV) and with the beam tilted 15°.

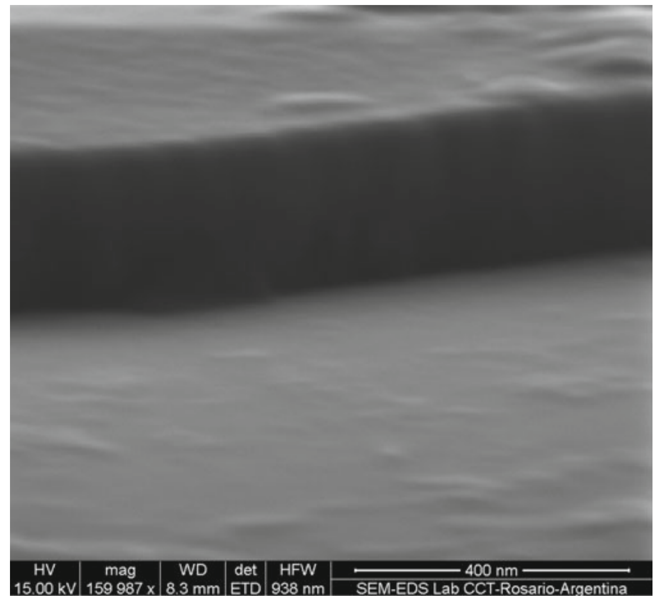


(a)

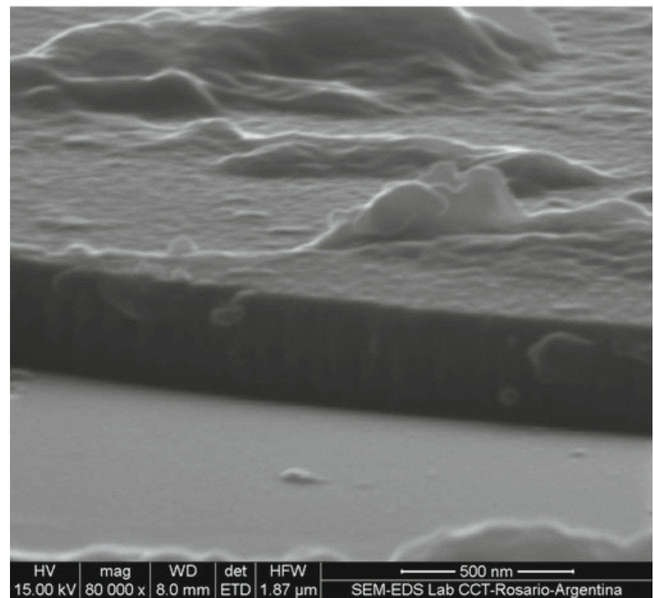


(b)

**Fig. 3.** Cross section SEM micrographs of the samples: (a) M0-20 and (b) M0-30.

The region labeled # 2, is mainly characterized by an intermixing of Al and Si. The composition of the interface and that of the first AlN atomic layers are dominated by a high Al content. The bulk $AlN_x$ is richer in N respect to the nominal composition of the AlN. Nevertheless, the bulk of the film is composed of AlN crystals, as observed through X-ray diffraction, but with an excess of nitrogen to the corresponding stoichiometric 50%/50% ratio for the compound. Indeed, we have observed a concentration Al/N ratio of ≈40%/60%. This nitrogen excess can be considered as absorbed by the AlN crystal structure [15]. In addition, the dependence of the vacancy content on

**Table 2.** Element concentration values in the different regions of M1-30 sample, as stressed in Figure 2. The different regions represent: substrate (label # 1); interface near the substrate (label # 2); the interface (label # 3); the first atomic layers of AlN near the substrate (label # 4); and bulk of deposited film.

| Label # | Si (at.%) | Al (at.%) | N (at.%) | O (at.%) | C (at.%) |
|---|---|---|---|---|---|
| 1 | 99.0 | – | – | 1.0 | – |
| 2 | 69.0 | 14.0 | – | 8.9 | 8.1 |
| 3 | 0.9 | 72.1 | 10.0 | 3.9 | 13.1 |
| 4 | 1.2 | 69.8 | 15.9 | 5.9 | 7.2 |
| AlN bulk | – | 37.0 | 63.0 | – | – |

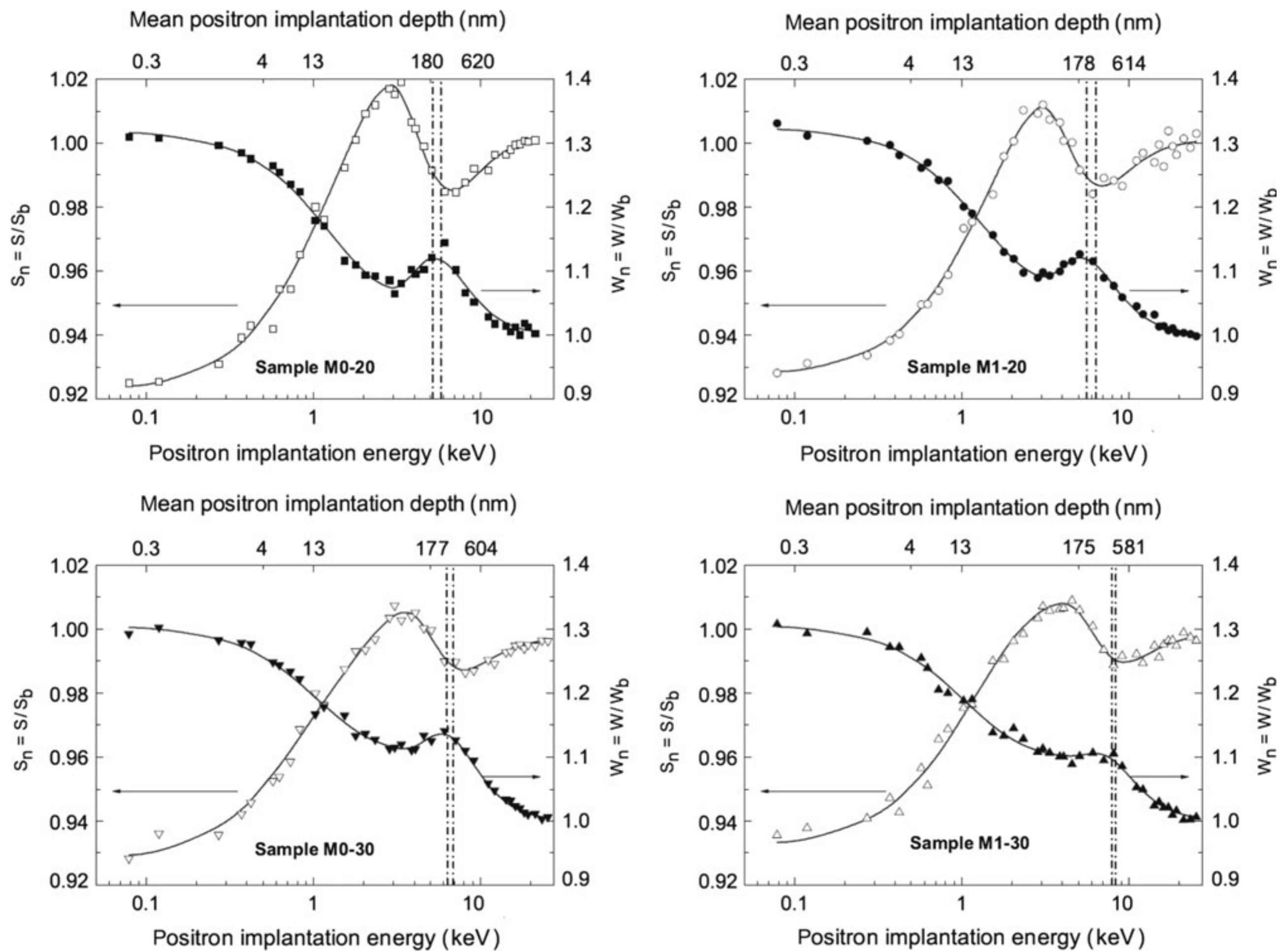


**Fig. 4.** Normalized line shape parameters $S_n$ and $W_n$ as a function of the positron implantation energy (bottom axis) and the mean positron implantation depth (top axis), for the four studied samples. Solid lines represent the best fit obtained using the VEPFIT program. The vertical dash-doted lines point out the film, the interface and the Si substrate, respectively.

the growth stoichiometry seems to be rather weak for low N excess [24].

The existence of C (almost in equal concentration along the whole studied profile) can be attributed to contamination of the films during deposition [25].

EDS results obtained for the M0-20, M1-20 and M0-30 samples do not significantly differ from those obtained for sample M1-30. Therefore, it can be concluded that the composition of the samples is not affected by the deposition time of the film.

In Figure 4, the depth profiling obtained by DBS for the different AlN samples are shown. For each sample the normalized line shape $S_n$ and wing $W_n$ parameters, respectively, as a function of the positron implantation energy, and the mean positron implantation depth are plotted.

To analyze the depth profiling of the different deposited samples, the experimental data were fitted using a procedure based on the solution of the stationary positron diffusion equation (VEPFIT program [26,27]).

**Table 3.** Characteristic parameters ($S_n$, $W_n$ and thickness) of the different layers as obtained from the VEPFIT analysis of the positron depth profiles. The errors associated with the $S_n$ and $W_n$ parameters are ±0.001 and ±0.002, respectively.

| Sample | Film characteristic parameters | | | Interface characteristic parameters | | |
|---|---|---|---|---|---|---|
| | $S_n$ | $W_n$ | $D$ (nm) | $S_n$ | $W_n$ | $D$ (nm) |
| M1-20 | 1.023 | 1.060 | 222 | 0.901 | 1.276 | 34 |
| M0-20 | 1.022 | 1.043 | 194 | 0.935 | 1.282 | 38 |
| M1-30 | 1.010 | 1.097 | 390 | 0.912 | 1.266 | 20 |
| M0-30 | 1.010 | 1.104 | 265 | 0.946 | 1.310 | 33 |

In all cases, data points could be well fitted considering the samples composed of three layers: the first layer was assumed to be the aluminum nitride film while the deepest one is the Si substrate. The intermediate layer was associated with the AlN film-Si substrate interface [11,28].

To fit the positron depth profiles, it is necessary to know the density or the thickness of the different layers [27]. For the Si substrate a density value of 2.33 g/cm$^3$ was assumed. In the case of the AlN and AlN-Si interface layers the densities were used as fit parameters taking advantage of the precise measurements by SEM of the thicknesses of each sample. As for the film as well as the interface, a same density value was found ($\rho = 3.0 \pm 0.2$ g/cm$^3$). In Table 3, the values of the pairs $S_n$ and $W_n$ characterizing the different layers obtained by the fitting procedure are reported. The following $S$ and $W$ values for bulk Si were obtained: $S_b = 0.551 \pm 0.001$ and $W_b = 0.148 \pm 0.002$.

For all AlN films very low positron diffusion lengths ($L_+$) were found. In the case of the M0-20 and M1-20 samples the obtained $L_+$ value was about 20 nm and for M0-30 and M1-30 samples $L_+$ was ≈10 nm. These values, an order of magnitude lower than the $L_+$ reported for Si monocrystal, indicate a strong positron trapping during its diffusion motion. Moreover, Saleh and Elhasi [27] stated that this $L_+$ reduction is provoked by dislocations and stacking faults in the columnar structure.

As can be seen in Table 3, the $S_n(W_n)$ values obtained for the interfaces are systematically lower (higher) than those characterizing the film; i.e., ≈0.90–0.95 versus ≈1.02 for the $S_n$ values and ≈1.26–1.31 versus ≈1.07 for the $W_n$ values. The values of the pairs $S_n$ and $W_n$ reflect positron annihilation with C [29], N and O [21,30] electrons. According to Brusa et al. [30] oxygen atoms develop vacancy formation in the surroundings. Furthermore, they configure open-volume defects in which the positron trapping process is improved [31]. On the other hand, Filip Tuomisto [24] stated that positron annihilation is higher in the vacancy-oxygen complex than in the vacancy-carbon one. It is important to mention that Druzhkov et al. [25] showed that C impurities reduced defect mobility and the positron annihilation in the vacancy-carbon complex developed was hindered. This result supports the statement from [24], assuring that the main annihilation mechanism is located in the vacancy-oxygen complex. As mentioned above, the presence of these elements in the interface was revealed from the EDS analysis.

On the other hand, at the interface a dependence of the $S_n$ values on the orientation of the Si substrate and the deposition time was observed. At each deposition time, the $S_n$ values for the interface of the film deposited on Si (1 1 1) are lower than those obtained for the films deposited on Si (1 0 0). Moreover, in the case of substrates with the same orientation the $S_n$ values for the samples deposited for a time of 20 min are lower than those deposited during 30 min. Specifically, for the samples deposited for 20 min, the $S_n$ value for the M1-20 sample was ≈0.90 while for the M0-20 sample this parameter was ≈0.93. In the case of the samples deposited for 30 min, the $S_n$ value for the M1-30 sample was ≈0.91 while the corresponding value for the M0-30 was ≈0.95. Taking into account that the increase of the $S_n$ values points out the presence of more open volume defects [30–32], these results would indicate that the deposition onto Si (1 0 0) substrates generates a more defective interface induced by the higher lattice mismatch between the AlN interface and the substrate [23,24,33]. Besides, it appears that an increase of the deposition time induces an increment of defects inside the interface. This increase is higher in the case of films deposited onto Si (1 0 0) substrates.

Regarding the AlN films, the information given in Table 3 shows that the pair of values $S_n$, $W_n$ for the same deposition time is almost equal. This means that the influence of the substrate orientation onto the growth of the film is lost. On the other hand, when comparing the results obtained for the different deposition times, a decrease in the corresponding $S_n$ values and a consequent increase in the $W_n$ values were observed, effect provoked by the film densification and the reduction of vacancy-oxygen complexes in the AlN film [31,34]. Mäki et al. [34] stated that in thin AlN films the aluminum vacancy ($V_{Al}$) – substitutional oxygen ($O_N$) complex, and not the isolated aluminum vacancies, is the main responsible of the positron trapping process and the subsequent annihilation. Thus, a vacancy-oxygen complex reduction will be translated to a decrease of $S_n$ values. Purposely, the $S_n$ value for the M1-20 and M0-20 samples was ≈1.02 while the $S_n$ value for the M1-30 and M0-30 samples was ≈1.01. This difference indicates that the films deposited for 20 min are more defected than those deposited for 30 min.

From the analysis of the results reported in Table 3, it can be concluded that the $S_n$ and $W_n$ values for the films studied are independent of the orientation of the Si substrate, because of the defective interface erased the

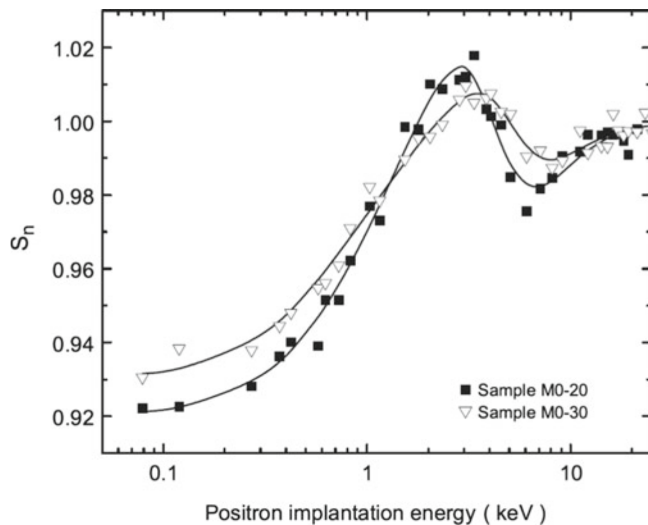


**Fig. 5.** Normalized line shape parameters $S_n$ as a function of the positron implantation energy for the M0 samples produced using two different times of deposition. Solid lines represent the best fit obtained using the VEPFIT program.

influence of the substrate. For a better comparison among samples prepared with two different deposition times, in Figure 5 the evolution of the shape parameter as a function of $E$ for the M0 samples is shown. From this figure and the $S_n$ values reported in Table 3, it can be concluded that the differences observed in the respective shape parameters can be attributed to a decrease of open volume defects [34] present inside the AlN films when the deposition time increases. Thus, this $S_n$ value was provoked only by dislocations, as stated in [27]. It is important to mention that the paper of Saleh and Elhasi had the focus on GaN thin films, but the structure behavior of this compound is qualitatively similar to the AlN thin films [24], compound described in the present paper.

## 4 Conclusions

From the results obtained in this work, it can be concluded that:

1. The columnar structure of the aluminum nitride films is independent of the deposition time of the well developed AlN crystalline structures.
2. The composition of all samples does not appreciably differ.
3. From positron analysis, it was possible to identify three different layers forming the AlN samples. These results are in very good agreement with those obtained using electron microscopy techniques.
4. The advantage to have direct measurements of the thicknesses of the layers from imaging techniques made it possible to estimate the density of the different layers from the fitting of the DBS depth profiles.
5. Inside the AlN films-Si substrate interfaces, different types of open volume defects were revealed. Specifically, it was found that positrons preferentially annihilate with carbon, nitrogen and oxygen electrons.
6. The defectivity of the interface depends on the orientation of the substrate: the interface is more defected when the film is grown on the Si (1 0 0) substrate with respect to that growth on the Si (1 1 1) substrate.
7. The defects in the bulk of the film are found to be independent of the orientation of the substrate. Besides, they decrease when the deposition time increases.

This work was partially supported by Agencia Nacional de Promoción Científica y Tecnológica (Argentina) (PICT 2011-1088 and PICT 2008-0374), Consejo Nacional de Investigaciones Científicas y Técnicas (Argentina) (PIP # 114-200801-00444), Ministerio de Ciencia, Tecnología e Innovación Productiva (Argentina)-Ministero degli Affari Esteri (Italy) (Project # 82/2010 and Project # IT/10/06) and Progetto CNR (Italy)/CONICET (Argentina) (Project 2010-2012 and Project # IT/10/06). Universidad de Córdoba (Spain) and ACIFIR Foundation (Argentina) were acknowledged, too. We want to express thanks to Mara Leonardi and Marco Bettonte for their technical help.

## References

1. N. Kumari, A.K. Singh, P.K. Barhai, Int. J. Thin Fil. Sci. Tec. **3**, 43 (2014)
2. S. Khan, S. Arya, P. Lehana, J. Nano- Electron. Phys. **5**, 02010 (2013)
3. M.A. Khan, Phys. Status Solidi A **203**, 1764 (2006)
4. M. Clement, L. Vergara, J. Sangrador, E. Iborra, A. Sanz-Hervás, Ultrasonics **42**, 403 (2004)
5. N. Onojima, J. Suda, H. Matsunami, MRS Proceedings **743**, L3.21 (2002)
6. N. Sinha, T.S. Jones, G. Zhijun, G. Piazza, J. Microelectromech. Syst. **21**, 484 (2012)
7. P.J. Stephanou, G. Piazza, C.D. White, M.B.J. Wijesundara, A.P. Pisano, Sens. Actuators A **134**, 152 (2007)
8. Y. Taniyasu, M. Kasu, T. Makimoto, Nature **441**, 325 (2003)
9. S. Stemmer, P. Pirouz, Y. Ikuhara, R.F. Davis, Phys. Rev. Lett. **77**, 1797 (1996)
10. M. Ishihara, S.J. Li, H. Yumoto, K. Akashi, Y. Ide, Thin Solid Films **316**, 152 (1998)
11. K. Ait Aissa, A. Achour, J. Camus, L. Le Brizoual, P.-Y. Jouan, M.-A. Djouadi, Thin Solid Films **550**, 264 (2014)
12. X.-H. Xu, H.-S. Wu, C.-J. Zhang, Z.-H. Jin, Thin Solid Films **388**, 62 (2001)
13. A. Kale, R.S. Brusa, A. Miotello, Appl. Surf. Sci. **258**, 3450 (2012)
14. A. Soltani, A. Stolz, J. Charrier, M. Mattalah, J.-C. Gerbedoen, H.A. Barkad, V. Mortet, M. Rousseau, N. Bourzgui, A. BenMoussa, J.-C. de Jaeger, J. Appl. Phys. **115**, 163515 (2014)
15. J. García Molleja, B.J. Gómez, J. Ferrón, E. Gautron, J. Bürgi, B. Abdallah, M.-A. Djouadi, J. Feugeas, P.-Y. Jouan, Eur. Phys. J. Appl. Phys. **64**, 20302 (2013)
16. A. Zecca, M. Bettonte, J. Paridaens, G.P. Karwasz, R.S. Brusa, Meas. Sci. Technol. **9**, 409 (1998)

17. C. Macchi, S. Mariazzi, G.P. Karwasz, R.S. Brusa, P. Folegati, S. Frabboni, G. Ottaviani, Phys. Rev. B **74**, 174120 (2006)
18. R.S. Brusa, G.P. Karwasz, N. Tiengo, A. Zecca, F. Corni, R. Tonini, G. Ottaviani, Phys. Rev. B **61**, 10154 (2000)
19. S. Valkealahti, R.M. Nieminen, Appl. Phys. A **35**, 51 (1984)
20. P. Asoka-Kumar, K.G. Lynn, D.O. Welch, J. Appl. Phys. **76**, 4935 (1994)
21. J. Yang, P. Zhang, E.Y. Lu, X.Z. Cao, R.S. Yu, B.Y. Wang, Nucl. Instrum. Meth. B **323**, 71 (2014)
22. Z.Q. Yao, Q. Ye, Y.Q. Li, Y.S. Zou, W.J. Zhang, S.T. Lee, Appl. Phys. Lett. **90**, 121907 (2007)
23. C. Caliendo, P. Imperatori, E. Cianci, Thin Solid Films **441**, 32 (2003)
24. F. Tuomisto, J. Phys.: Conf. Ser. **265**, 012003 (2011)
25. A.P. Druzhkov, D.A. Perminov, V.L. Arbuzov, J. Nucl. Mater. **434**, 198 (2013)
26. A. van Veen, H. Schut, J. de Vries, R.A. Hakvoort, M.R. Ijpma, AIP Conf. Proc. **218**, 171 (1990)
27. A.S. Saleh, A.M. Elhasi, Am. J. Modern Phys. **3**, 24 (2014)
28. F. Engelmark, J. Westlinder, G.F. Iriarte, I.V. Katardjiev, J. Olsson, IEEE Trans. Electron Devices **50**, 1214 (2003)
29. N. Laidani, G. Speranza, L. Calliari, R.S. Brusa, S. Mariazzi, in *Cold Plasma for Thin Film Deposition: Processes, Characterizations and Applications*, edited by E. Tomasella (Research Signpost, Kerala, India, 2010)
30. R.S. Brusa, W. Deng, G.P. Karwasz, A. Zecca, D. Pliszka, Appl. Phys. Lett. **79**, 1492 (2001)
31. I. Makkonen, C. Rauch, J.-M. Mäki, F. Tuomisto, Physica B **407**, 2684 (2012)
32. C. Rauch, I. Makkonen, F. Tuomisto, Phys. Rev. B **84**, 125201 (2011)
33. T. Ogawa, M. Okamoto, Y.Y. Khin, Y. Mori, A. Hatta, T. Ito, T. Sasaki, A. Hiraki, Diamond Rel. Mater. **6**, 1015 (1997)
34. J.-M. Mäki, I. Makkonen, F. Tuomisto, A. Karjalainen, S. Suihkonen, J. Räisänen, T.Y. Chemekova, Y.N. Makarov, Phys. Rev. B **84**, 081204(R) (2011)